INTERNAL LEAKAGE MONITORING OF TELESCOPIC HYDRAULIC CYLINDER

M.Tech. Thesis

By
SIDHARTHA KHARE
(180003054)

DEPARTMENT OF MECHANICAL ENGINEERING
INDIAN INSTITUTE OF TECHNOLOGY INDORE
JUNE 2023

INTERNAL LEAKAGE MONITORING OF TELESCOPIC HYDRAULIC CYLINDER

A THESIS

Submitted in partial fulfillment of the
requirements for the award of the degree
of
Dual Degree (B.Tech + M.Tech)

by
SIDHARTHA KHARE

DEPARTMENT OF MECHANICAL ENGINEERING
INDIAN INSTITUTE OF TECHNOLOGY INDORE
JUNE 2023

INDIAN INSTITUTE OF TECHNOLOGY INDORE

CANDIDATE'S DECLARATION

I hereby certify that the work which is being presented in the thesis entitled **INTERNAL LEAKAGE MONITORING OF TELESCOPIC HYDRAULIC CYLINDER** in the partial fulfillment of the requirements for the award of the degree of **DUAL DEGREE (B.TECH + M.TECH)** and submitted in the **DEPARTMENT OF MECHANICAL ENGINEERING, Indian Institute of Technology Indore**, is an authentic record of my own work carried out during the time period from August 2021 to June 2023 under the supervision of **Dr. Pavan Kumar Kankar, Associate Professor, Department of Mechanical Engineering, Indian Institute of Technology Indore** and **Dr. Ankur Miglani, Assistant Professor, Department of Mechanical Engineering, Indian Institute of Technology Indore**.

The matter presented in this thesis has not been submitted by me for the award of any other degree of this or any other institute.

Siddhartha
05-06-23

Signature of the student with date
(SIDHARTHA KHARE)

This is to certify that the above statement made by the candidate is correct to the best of my/our knowledge.

05/06/23

(Dr. PAVAN KUMAR KANKAR)

(Dr. ANKUR MIGLANI)

SIDHARTHA KHARE has successfully given his/her M.Tech. Oral Examination held on **25th May 2023**.

Signature(s) of Supervisor(s) of M.Tech. thesis
Date: 05/06/23

Convener, DPGC
Date: 05/06/23

Girish

Signature of PSPC Member #1
(Dr. Girish Chandra Verma)
Date: 05/06/23

05.06.2023

Signature of PSPC Member #2
(Dr. Ram Bilas Pachori)
Date:

ACKNOWLEDGEMENT

First and foremost, I would like to take this opportunity to express my sincere gratitude to my esteemed supervisors, **Dr. Pavan Kumar Kankar** and **Dr. Ankur Miglani** for their guidance and mentorship throughout the duration of my two-year Masters of Technology program. Their valuable feedback and constructive criticisms helped me improve my work. I would also like to extend my thanks to my PSPC members **Dr. Girish Chandra Verma** and **Dr. Ram Bilas Pachori** for their insightful feedback, suggestions, and contributions to the project's growth.

I am grateful to Dr. Jatin Prakash whose guidance and inputs have been helpful in shaping my understanding of the subject matter. I would like to further extend my gratitude towards my laboratory colleagues: Dr. Vinod Singh Thakur (PhD), Dr. Nagendra Singh Ranawat (PhD), Mr. Apoorv Tripathi (PhD), Mr. Anurag Pathak and Mr. Deepak Kumar for their constant encouragement, camaraderie, and moral support throughout my project.

I am deeply indebted to my parents and my sister for their unwavering love, encouragement, and support. Their belief in me and their constant motivation have been a driving force behind my success.

Lastly, I would like to express my heartfelt gratitude to all those who have contributed, directly or indirectly, to my journey.

With Regards,

Sidhartha
05-06-23

Sidhartha Khare

ii

Abstract

Hydraulic telescopic cylinders are commonly used in industry for various applications and are often subjected to high-pressure working conditions. This makes continuous monitoring for internal leakage in telescopic cylinders necessary to accurately characterize the health of hydraulic systems and maintain their efficiency and safety as failure can have costly and even fatal consequences. In this study, a hydraulic telescopic cylinder test rig with a maximum pressure of 210 bars is employed to simulate internal fluid leakage in a two-stage telescopic cylinder. Internal leakage is introduced by grinding the seals using a table-top grinding wheel. The trends in the pressure signals from the telescopic cylinder and their relation with the pressure signals from the loading cylinder are studied. The ratio of pressures in the two cylinders is found to be equal to the inverse ratio of their cross-sectional areas. The effect of increasing wear on the pressure signals is also explored. Statistical time domain features are extracted from the pressure signals from the two chambers of telescopic cylinder. The features are ranked in decreasing order of their importance by using feature ranking methods such mean decrease in impurity and permutation importance and top eight features are identified. Four machine learning classifiers, namely, Random Forest, SVM, logistic regression and gradient boosting classifiers are developed and trained on these features to automatically detect and categorize internal fluid leakage into proper leakage severity level. A comparison is made between the classification accuracies of the four algorithms and it is observed that Random Forest classifier is the most accurate.

TABLE OF CONTENTS

LIST OF FIGURES

x

LIST OF TABLES

NOMENCLATURE

$A_{\mathrm{l,r}}$	Cross-section area at which fluid pressure acts as it fills in the rear chamber of loading cylinder
$A_{t,\mathrm{r}}$	Cross-section area at which fluid pressure acts as it fills in the rear chamber of telescopic cylinder
$p_{\mathrm{l,r}}$	Pressure in the rear chamber of loading cylinder
$p_{t,\mathrm{r}}$	Pressure in the rear chamber of telescopic cylinder

ACRONYMS

DAQ	Data Acquisition System
DCV	Directional Control Valve
EMD	Empirical Model Decomposition
FCM	Fuzzy C-means
FMEA	Failure mode and effects analysis
GB	Gradient Boosting
HHT	Hilbert Huang Transform
HMI	Human Machine Interface
IMF	Intrinsic Mode Functions
LVDT	Linear Variable Differential Transformer
MDI	Mean Decrease in Impurity
MLP	Multilayer Perceptron
PPRV	Proportional Pressure Relief Valve
RF	Random Forest
RFE	Recursive Feature Elimination
RMS	Root mean square
RUL	Remaining useful life
SVM	Support Vector Regression

Chapter 1: Introduction

Telescopic cylinders, also called as telescoping or multi-stage cylinders, are hydraulic cylinders that comprise multiple tubes made of steel or aluminum. These tubes, nested within one another, have decreasing diameters from the outermost to the innermost. Each tube is known as a stage. The stage with the largest diameter is referred to as the main stage or barrel, and the smallest diameter stage referred to as the plunger.

Compared to the typical single stage hydraulic cylinder, telescopic cylinders have a number of advantages primary of which is their capability to provide a very long stroke while having a compact design. This enables it to reach greater distances without the need for excessively long cylinders. They have a nested tube construction, which allows it have a compact overall size when retracted. Depending on how many stages are in the telescopic cylinder, the retracted length typically ranges between 20-40% of the fully extended length which makes it ideal for use in applications where limited space is an issue, such as in mobile equipment or tight working environments. Further, due to their ability to extend and retract individual stages, telescopic cylinders provide flexibility in adjusting the working length. This allows for precise positioning and optimizing the stroke length for specific tasks. Telescopic cylinders are capable of handling a wide array of loads and applications, from light-duty tasks to heavy-duty. Their nested tube design provides the necessary strength and stability, allowing it for versatile use in a variety of industries.

Telescopic cylinders are widely used in many different industries, including construction, agriculture, material handling, and transportation, due to their advantages. They are employed in a diverse range of equipment and systems, such as aerial work platforms, hydraulic excavators, telescopic

handlers, dump trailers, missile launchers, aircraft landing mechanism and more.

However, they also have some disadvantages compared to single-stage hydraulic cylinders. They have a more complex design compared to single-stage cylinders since they consist of multiple nested stages, which require precise alignment and sealing. This complexity usually results in higher manufacturing costs and maintenance challenges. Their nested design can also cause them to have reduced rigidity and increased deflection under heavy loads which limits their load-bearing capabilities. Thus, telescopic cylinders are primarily used in applications where the piston bears minimal side loading. Further, with the presence of multiple stages and sealing points, telescopic cylinders may have a higher risk of hydraulic fluid leakage compared to single-stage cylinders especially under high-pressure applications. Proper sealing and maintenance are essential to minimize this risk.

1.1 Construction of a telescopic cylinder

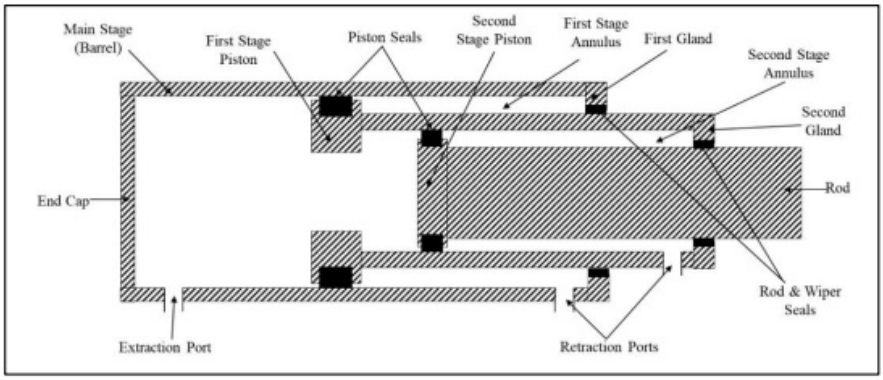

Fig 1.1: Schematic diagram of a 2-stage double-acting telescopic hydraulic cylinder

Fig 1.1 shows the schematic diagram of a cut section of a double-acting 2-stage telescopic hydraulic cylinder with internal construction and fluid passage. The largest diameter cylinder, known as the main stage or barrel, forms the outermost part of the telescopic cylinder. It provides structural support and houses the inner stages. The main stage is usually made of durable materials such as steel or aluminum to withstand the forces and pressures involved. Nested within the main stage are the two inner stages, which are cylinders of successively smaller diameters. Each inner stage has two components: a piston and a piston rod. The piston rod of every stage except the smallest stage is hollow. The piston rod of the smallest stage is simply called rod or the plunger.

The end cap is the component located at one end of the telescopic cylinder. It is also sometimes referred to as the base or head of the cylinder. It is typically a solid or threaded structure that serves as a closure for the cylinder and houses various internal components. The end cap provides a mounting point for the cylinder and helps to maintain the structural integrity of the cylinder assembly. It is designed to withstand the forces and pressures generated during operation.

The gland is located at the opposite end of the cylinder from the end cap. It serves as a housing for the sealing system that prevents leakage of hydraulic fluid and maintains the integrity of the hydraulic system. It contains the seals, O-rings, or other sealing elements that ensure a tight and reliable seal between the stages of the telescopic cylinder. The gland also provides support and guidance for the movement of the nested stages within the cylinder. Oil transfer holes are present in the annulus region which allow the working fluid to travel from one annulus region to the next if separate retraction ports are not provided at each stage. [1]

The piston of each stage is fitted with a guide ring and a piston seal. The guide ring helps absorb radial loads and maintain the axial alignment of the piston rod. The piston seals prevent the fluid from crossing from one side of the piston to another. The gland side of the stages contain wiper seals, rod seals and guide rings. The wiper seal prevents the transmission of contaminations from the outside of the cylinder to inside. The rod seals ensure that the working fluid remains contained within the cylinder and does not leak out.

1.2 Types of telescopic cylinders

Depending on whether the telescopic cylinder can actuate in both directions, telescopic cylinders can be classified into two types [2]:

i. **Single-acting telescopic cylinders**: They have a single hydraulic port, usually for extraction, and are actuated in one direction. The working fluid enters from the port and exerts pressure on the piston from the end cap side due to which the cylinder extends. Usually, the 1st stage of the cylinder extends first, followed by progressively smaller pistons, but the order in which they extend depends on dimensions and design of the telescopic cylinder. Single-acting telescopic cylinder rely on external forces, usually gravity, for retraction. They are often used in applications where there is always some load acting on the cylinder such as dump trucks, cranes, and material handling equipment.

ii. **Double-acting telescopic cylinders:** Double-acting telescopic cylinders have hydraulic ports at both ends and can be actuated in both directions. Depending on the location of extraction and retraction ports, they can be divided into further 3 types. In the first type, the extraction port is located on the main stage and the retraction port on the plunger. Multiple retraction ports, one on each

stage, can also be present as shown in Fig 1.1. In the second type, both ports are located on the plunger in which case the plunger is hollow and in the third type both are located on the main stage. Each design type has its own advantages and disadvantages but the basic working is the same.

The extraction mechanism is similar to that of a single acting telescopic cylinder. Double acting telescopic cylinders are retracted by pressuring the space between outer diameter of the current stage and inner diameter of the next larger stage i.e., the annulus space. Under the fluid pressure exerted on the piston from the gland end side, that stage completely retracts and a pathway i.e., the oil transfer hole to the annulus space of the next larger stage from that of the current stage then becomes open and the process repeats. In this way, the cylinder completely retracts. [1]

1.3 Thesis organization

The following is a chapter-by-chapter breakdown of the current work:

Chapter 1 deals with the introduction of the telescopic cylinder, its advantages and disadvantages compared to a single stage hydraulic cylinder, its applications in industry and the types of telescopic cylinders. The working of the telescopic cylinder is also explained in brief. At the end, the organization of the various chapters in the thesis is mentioned.

Chapter 2 discusses the past published work related to telescopic cylinders. First, the common causes of failures of telescopic and hydraulic cylinders are discussed followed by a discussion on the various maintenance strategies employed in the industry to prevent and minimize the failures. In the last section of the chapter, the various condition-monitoring methods

developed in literature are discussed and the significance and scope of current study is mentioned

Chapter 3 introduces the experimental facility used in this study and explains its working in detail. The second half of the chapter discusses the relations between the various pressure signals obtained through the data acquisition system and explains the behaviours in the pressure signal plots.

Chapter 4 briefly explores the effect of increasing seal wear on the pressure signals and discusses in detail the methodology used to develop four machine learning classifiers for monitoring internal fluid leakage. The classification accuracies of the four models is compared.

Chapter 5 concludes and summarizes the current research work. A brief idea of the applications of current work and future scope is also discussed.

Chapter 2: Literature Survey

2.1 Introduction

Telescopic cylinders are widely used in hydraulic systems for applications such as construction equipment, material handling, and industrial machinery. Despite their importance, these cylinders are susceptible to various faults that can adversely affect their performance, reliability, and lifespan. Understanding and identifying common faults in telescopic cylinders is crucial for efficient maintenance, timely repairs, and overall system integrity. The various faults commonly observed in industry are:

1) Fluid Leakage: One of the most prevalent faults in hydraulic and telescopic cylinders is fluid leakage. According to Johny et al. [3] approximately 42% of all problems in hydraulic systems arise due to fluid leakages. Fluid leakage can be classified into two types: internal leakage and external leakage [4]. Internal leakage occurs within the cylinder itself. It involves fluid bypassing the normal flow path and leaking from the high-pressure side of the cylinder to the low-pressure side or vice versa, without exiting the cylinder to the external environment.

Internal leakage can happen due to worn seals, damaged piston or rod surfaces, inadequate lubrication, or improper fluid flow control. It can result in reduced cylinder efficiency, decreased force or load-holding capacity, and potential instability in the hydraulic system [5][6].

External leakage refers to the escape of hydraulic fluid from the hydraulic cylinder to the surrounding environment. It occurs when there is a breach in the cylinder's seals, gaskets, or other components that are designed to contain the fluid within the system [8]. This type of leakage not only leads to a loss of fluid but can also result in environmental contamination, reduced

system performance, and risk of injury, risk of health problems and risk of fire hazards. [5][7].

In hydraulic cylinders, fluid leakage can occur due to number of factors such as seal defects, quality of product assembly, design considerations, casting imperfections, machining defects, and other related factors. [9]

Approximately 66% of all leakages are caused by seal defects [9]. Seal defects can arise from various factors, including the aging of seal material, dimensional changes caused by temperature and humidity fluctuations, contamination of fluid, and high operating load and pressure [10]. Examples of seal defects include seal hardening, scarring, seal extrusion, seal wear etc. Fluid leakage due to defects during product assembly account for 17% of total fluid leakages and that due to casting, machining or design defects account for 14% of all fluid leakages [9]. Failure to replace a seal in a timely manner can result in fluid leakage or fluid contamination by seal particles or particles from the surrounding environment such as dust, water, dirt etc.

2) Piston misalignment: It is another relatively common fault in telescopic cylinders. It can result from improper installation, mechanical stress, or wear over time. Piston misalignment can cause uneven wear, increased friction, and reduced operational efficiency [12].

3) Fluid contamination: Fluid contamination is a frequent issue in hydraulic systems, including telescopic cylinders. Contaminants such as dirt, moisture, air, or metal particles can enter the system, leading to accelerated wear, seal degradation, and reduced component lifespan. Presence of moisture can affect and change physical and chemical properties of the fluid. Its presence alters physical properties of the fluid such as its viscosity, its load-carrying capacity and its power-transfer characteristics and provides a conducive environment for oxidation and

corrosion which can result in deposition of sludge [13][14]. Particle contamination in fluids is responsible for a large percentage of failures in hydraulic systems [15]. Harder particle contaminants such as metal particles can cause significant damage by scratching the seals of hydraulic cylinders or creating scores on metal surfaces. Softer particle contaminants such as fiber and textile particles can result in blockage of the hydraulic control elements such as orifices, valves, ports, and filters. Thus, particle contaminants degrade the fluid quality, clog filters, ports, valves, and damage components, leading to reduced system performance, reduced component lifespan and increased maintenance requirements. Particle components which have very small particle sizes are highly abrasive and thus can cause significant damage to the components of the hydraulic system if they are present in sufficient quantity. According to [16], of all component failures in hydraulic components, 90% are due to surface fatigue and abrasive wear caused by particle contaminants.

4) Cylinder Drift: Cylinder drift refers to the unintended movement or creeping of telescopic cylinders when the system is inactive. It can be caused by internal leaks, valve malfunctions, or improper control system adjustments. Internal leakage disrupts the balance of forces within the cylinder, leading to drift. Malfunctioning valves in the hydraulic system can contribute to cylinder drift. Control valves or directional valves play a critical role in regulating fluid flow and pressure. If these valves do not function correctly, they may not completely block fluid flow or maintain proper pressure, causing unintended movement of the cylinder. Valve issues can include improper seating, valve spool leakage, or valve stiction [17][18]. Incorrect pressure settings, inadequate flow control, or suboptimal adjustments of pressure regulators, flow control valves and proportional valves can cause instability in the system. This instability can result in uncontrolled fluid flow, leading to cylinder drift. Excessive external loads applied to the cylinder can cause drift. When the cylinder is designed to hold

a specific load, adding additional loads or imbalanced loading can create additional forces on the cylinder. These forces can overcome the holding force of the hydraulic system, causing the cylinder to move gradually over time. Cylinder drift affects the accuracy and stability of the system [19][20][21].

5) Rod Scoring or Surface Damage: Scoring or surface damage refers to the formation of scratches, grooves, or marks on the surface of the rod of telescopic cylinders. It can occur due to abrasion, corrosion, insufficient lubrication, or foreign particle intrusion. One of the primary causes of rod scoring is the presence of contaminants in the hydraulic system which act as abrasives, causing scratches and scoring when the rod moves within the cylinder. Inadequate lubrication can also cause rod scoring. Insufficient lubrication increases the friction between the rod and the cylinder wall, resulting in metal-to-metal contact. This contact can cause the rod surface to become scratched and scored over time. Neglecting proper maintenance practices, such as inadequate cleaning of the system or rough handling of the hydraulic cylinder, can contribute to rod scoring. Poor maintenance allows contaminants to accumulate and increases the risk of damage to the rod surface. Rough handling can cause external impacts or scratching, leading to scoring. Such damage can result in increased friction, seal wear, and reduced system efficiency [22][23].

6) Bent Rods or Cylinders: External impact, overloading, or mishandling can cause bending of the rod or cylinder in telescopic cylinders. Bent components can lead to uneven loading, increased friction, and limited stroke length.

2.2 Monitoring of hydraulic cylinders

Failures in hydraulic cylinders are mostly due to fluid leakage and contamination. Apart from any structural damage to the hydraulic cylinder, it is not easy to determine the condition of the fluid, seal, or other components of the hydraulic cylinder through visual inspection alone without first partially or completely disassembling the hydraulic system. Unexpected failures increase maintenance cost, might cause damage to other components of the hydraulic system, reducing the operation availability and result in expensive repairs or replacement of critical components which can have significant financial consequences [24][25][26].

Different maintenance strategies can be used to lower costs both financially and operationally and to improve the safety and reliability of the system. Conventional maintenance strategies that are used in industry are reactive or breakdown maintenance, proactive or reliability centered maintenance and preventive or time-based maintenance [27]. Reactive maintenance involves repairing or replacing hydraulic components only when they fail or break down. This approach relies on reactive responses to equipment failures and typically involves minimal planned maintenance. While this approach may be suitable for non-critical systems or low-cost components, it can result in unexpected downtime, higher repair costs, and potential safety risks [28].

Preventive maintenance involves performing routine inspections, servicing, and component replacements at predefined regular time intervals. This strategy is carried out in a fixed time intervals, such as weekly, monthly, or annually, regardless of the actual condition of the hydraulic system. This helps identify potential issues early on, but it may also result in unnecessary

maintenance actions and costs if components are still in good condition [28][29].

Reliability based maintenance involves conducting risk assessments, analyzing failure data, and prioritizing maintenance tasks based on the criticality of components and uses techniques like failure mode and effects analysis (FMEA) to minimize downtime and improve system reliability [30].

Predictive maintenance, also known as condition-based maintenance is an alternative to conventional maintenance. It relies on real-time monitoring and analysis of key parameters to predict the condition of hydraulic components [31]. It involves using sensors, data analysis, and condition monitoring tools to track parameters like temperature, pressure, vibration etc. and based on the values of these parameters, maintenance activities are scheduled. Thus, maintenance of components is performed only when required [32][33]. While the initial cost of implementation of condition-based monitoring may be considerable initially, it can be offset in the long run through savings on maintenance cost. Maintenance cost and cost associated with sudden failure of equipment can be substantially reduced by implementing predictive maintenance strategies for hydraulic systems [34]. Using real-time condition data enables the operator to schedule maintenance activities depending on the equipment health thereby eliminating unplanned maintenance time [35].

The health of a telescopic cylinder can be monitored directly or indirectly. Direct methods include visual inspection of the components or measuring deviations in the dimension of the components. Since most components of the hydraulic cylinder are concealed within it, it is difficult to implement these methods and involves partial or complete disassembly of the system which reduces the availability of the system. Further, implementing visual

inspection methods such as computer vision are not economically feasible [36].

Indirect monitoring methods involve measuring parameters or characteristics that are related to the performance or behavior of the components but are not directly measured on the components themselves. For a hydraulic system, these parameters can be pressure, temperature, vibration, chemical and physical properties of the working fluid etc. [37]

2.3 Condition monitoring of fluid leakage

Numerous methodologies have emerged for detecting fluid leakage in hydraulic and telescopic cylinders effectively, by monitoring parameters such as pressure, temperature, acoustic emission, vibration, and torque [38]. These parameters can be monitored using various sensors such as pressure and temperature sensors, accelerometers, acoustic emission sensors and torque sensors. To analyze the data obtained from these sensors, various signal processing techniques can be used such as time-domain analysis, frequency-domain analysis, and time-frequency analysis.

Whenever there is leakage in the hydraulic cylinder, there is a pressure drop in the chamber due to loss of fluid. This pressure drop can be read using hydraulic pressure sensors indicating the presence of a leak. Hydraulic pressure sensors measure pressure in the hydraulic system and give analog electrical signals as output. There are several studies which have attempted to detect fluid leakage using wavelet analysis by monitoring pressure signals from hydraulic cylinders. Wavelet analysis involves decomposing a signal into a set of basis functions called wavelets which are localized in both time and frequency domains [39]. Goharizzi and Sepehri (2009) [40] applied wavelet transformation to detect internal fluid leakage in hydraulic actuators due to damaged seal. The hydraulic actuator was not subjected to

any load and to detect healthy and faulty conditions, the root mean square (RMS) of the level 2 detail coefficient was used as an indicator since its magnitude dropped in presence of fluid leakage. In [42], the same method was applied to detect leakage in a single stage hydraulic actuator under load and RMS of level 2 detail coefficient was again found to be sensitive to internal fluid leakage. In [41], wavelet transform was used for detecting external fluid leakage in hydraulic actuators. RMS of level 4 detail coefficient was shown to be responsive to external leakage with its value decreasing as the leakage increased and was thus used as an indicator to detect leakage. Zhao et al. [42] used wavelet packet analysis to detect different fluid leakage levels. The energy variance of wavelet packets was found to be the most sensitive, in comparison to other features, to fluid leakage. [43] applied wavelet transforms to the pressure signal, and the energy of the different frequency bands was calculated in eigenvector form after wavelet decomposition. These eigenvectors were then input to train a backpropagation neural network to detect fluid leakage in hydraulic cylinders. [44] applied Hilbert Huang Transform (HHT) on the pressure signals to monitor internal fluid leakage. The pressure signals were first broken into intrinsic mode functions (IMFs) using the empirical mode decomposition (EMD) technique. The instantaneous amplitudes and frequencies of the IMFs were then obtained by applying the Hilbert transform. It was found that internal fluid leakage was sensitive to the instantaneous magnitude of the first IMF.

Sharifi et al. [45] implemented support vector machine (SVM) with a linear kernel to detect internal fluid leakage due to damaged seal and component wear. The peaks of the pressure signals were used to extract features such as location, width and height of the pressure peaks which reduced its dimensionality significantly. These features were then used to train the SVM. Lu et al. [46] used a fault diagnosis method for axial piston pumps combining a two-step EMD along with fuzzy C-means (FCM) clustering.

Hilbert marginal energy spectrum was calculated locally each IMF obtained from the two-step EMD method and corresponding features vectors were obtained which was then used in FCM algorithm. To measure the degradation in bearing performance, Rai et al. [47] suggested an indicator based on a self-organizing map. Support vector regression was used to estimate the remaining useful life (RUL) of the bearings. Ramachandra et al. [48] monitored fluid leakage caused by degradation of rotary seals by implementing a multilayer perceptron (MLP) neural network. Time-domain features were extracted from the friction torque signal. Recursive feature elimination (RFE) was used to identify the features that contribute the most to predictive accuracy and ranked RMS, mean, SRA and breakout torque as the optimal feature subset. 10-fold cross validation was implemented to prevent overfitting. The classification accuracy of the MLP neural network model was compared with and observed to be higher than logistic regression and random forest models. Prakash (2022) [54] developed a high-pressure (210 bar) hydraulic test rig actuated by a 2-stage hydraulic cylinder. The test rig can simulate various loading motions such as ramp loading, square loading, semisoidal loading and triangular loading. A leakage detection algorithm was developed based on transductive semi-supervised SVM (TS-SVM) which was able to classify the internal leakage with 100% accuracy.

Cerrada et al. [49] designed a system to diagnose spur gears faults using a two-step approach. First, several time-domain features, frequency-domain features and wavelet transform features were obtained from the vibration signal and following which a genetic algorithm was used to identify the optimal feature subset. Random forest model was used to monitor and diagnose different fault levels in spur gears. 179 classifiers were trained on 121 datasets by Fernández-Delgado et al. [52] and compared their accuracy and efficiency. It was observed that Random Forest (RF) performed the best on most of the datasets. Verikas et al. [50] conducted a comparative analysis of the accuracy and complexity of Random Forest (RF) and other commonly

used classification algorithms in various domains, based on extensive research findings available in the public literature. The results demonstrated that RF consistently outperformed other techniques, irrespective of whether the number of variables was large or small. Furthermore, instances where RF was outperformed by other algorithms were relatively scarce. Chawte [51] compared several classification algorithms such as OneR, ZeroR, J48, PART, Naive Bayes and Random Forest for condition monitoring of hydraulic systems. The algorithms were trained on time-domain features. Random Forest was observed to have the highest accuracy followed by J48 algorithm. Studies focused on the monitoring and detection of fluid leakage (internal) such as that by Li et al. [53] have used random forest classifier for this purpose to get significant results. IMFs of inlet pressure, outlet pressure and pressure difference were obtained by EMD method. Characteristic features of IMFs were calculated and were used for training the random forest classifier. Random Forest algorithm's classification accuracy was observed to be higher than that of the SVM algorithm trained with wavelet features.

It is clear from the above literature survey that internal fluid leakage is a major reason behind failures in hydraulic cylinders and thus it is important to minimize it. Implementing maintenance strategies can help reduce these failures. Condition-monitoring based maintenance strategies are becoming popular as they allow real time monitoring of parameters of hydraulic systems and thus maintenance activities can be planned in a more efficient manner. There have been several studies which have used signal processing techniques and data-driven methods for detecting internal leakage in hydraulic cylinders. However, most of these studies have focused on internal leakage in single stage hydraulic actuators. Further, these studies have used artificial ways to simulate leakage and thus overlooks the actual conditions of internal leakage in hydraulic cylinders.

In this study, we will introduce leakage fault of different severities in a 2-stage hydraulic telescopic cylinder in a specially designed test rig that is capable of simulating various types of real-life loading scenarios. The leakage is introduced by wearing the piston seal on the 1st stage or intermediate stage of the telescopic cylinder. Using pressure sensors, pressure data is obtained from both chambers of the telescopic cylinder while it completes one cycle of extraction and retraction. Statistical time domain features are calculated from the pressure signal data and feature ranking methods are used to find the most relevant features. Four machine learning models are trained on the dataset and their classification accuracies are compared.

18

Chapter 3: Experimental Setup and Working

3.1 Introduction

To study the effects of internal fluid leakage in telescopic cylinders, a specially designed high-pressure (210 bar) hydraulic telescopic cylinder experimental test facility is used. The experimental facility is capable of replicating real-world loading conditions such as ramp wave loading, square wave loading, impulse loading etc. Using various sensors such as pressure, temperature, and flow rate sensors, we can monitor different parameters of the hydraulic system.

3.2 Experimental Facility

The hydraulic experimental facility consists of a 2-stage telescopic hydraulic cylinder which is the cylinder under test and a single stage hydraulic cylinder which acts as the loading cylinder. The flow in the hydraulic facility is created by a fixed displacement (external geared) pump driven by an electric motor. The hydraulic fluid used in the circuit is HP ENKLO 68. The fluid is stored in a reservoir which consists of filters and filler breather to maintain the quality of oil and allow the flow of clean air between the reservoir and surroundings thus maintaining atmospheric pressure inside the reservoir. The amount of oil in the reservoir is also indicated on one of the sides of the reservoir by an indicator which is connected to a float. An unloading cum safety pressure relief valve set at a maximum pressure of 210 bar ensures the safety of the system.

A 4/3 directional control valve(DCV) controls the flow to the telescopic cylinder while the flow to the loading cylinder is controlled by a proportional pressure relief valve and a 4/3 DCV. There are many sensors in the experimental facility such as pressure sensors, temperature sensor,

load cell, LVDT and flow meters which allow us to monitor parameters such as pressure in both the chambers of the telescopic cylinder (rod-end and cap-end), pressure in the two chambers of the loading cylinder, flow rate, temperature of the hydraulic fluid, the position of the telescopic cylinder, and the load acting on it.

Data is acquired using a data acquisition (DAQ) system which is of HYDAC make. The whole setup is controlled by an electrical panel which contains a HMI display and custom PLC code. The electrical panel consists of various predefined input loading signals such as ramp wave, square wave, triangular wave etc.

3.3 Working of the experimental facility

The electric motor mounted on top of the reservoir is the prime mover which drives the fixed displacement pump due to which flow is created in the circuit. The hydraulic oil rises from the reservoir, passes through a pressure line filter with filtration capacity of 25 microns, and reaches the unloading cum safety relief valve which is set at a pressure of 210 bars. If the pressure in the circuit rises above this limit, the safety relief valve bypasses the flow back to the reservoir after passing through the air cooler system and return filter bar. If the pressure in the circuit is below this safety limit, the fluid flows through another filter (check details in lab), a flow control valve and an electronic flow rate transmitter which allows the measurement of flow rate, temperature and pressure. The fluid reaches a junction from where it splits and flows towards two different 4/3 directional control valves (DCVs). One DCV is responsible for controlling the flow to the telescopic cylinder while the other is responsible for controlling the flow to the loading cylinder.

The ports A and B of the 4/3 DC valve controlling the flow to the telescopic cylinder are connected to the two ports of the telescopic cylinder - one at the cap-end side of barrel (port A) and one at the rod-end side of the first stage (port B2). One more port (port B1) is provided at the rod-end side of the cylinder barrel to provide a uniform flow of oil to the two stages of the telescopic cylinder during retraction. During the extraction stroke, the fluid flows from the valve to the port A of the telescopic cylinder and from ports B1 and B to the return line via the valve. During the retraction stroke, the fluid flows from the valve to ports B1 and B2 of the telescopic cylinder and from port A of the telescopic cylinder to the return line via the valve.

The DC valve controlling the flow to the loading cylinder is connected to a proportional pressure relief valve (PPRV) and the loading cylinder. Oil from the DC valve flows to the PPRV as well as the loading cylinder. If the PPRV is open, oil flows back to the tank via the return line. If it is closed, the pressure starts building up in the loading cylinder. The PPRV is used to proportionally control the pressure according to the loading signal input in the electrical panel by changing the current in the solenoid. The primary port of the PPRV is connected to the DC valve while the secondary port is connected to the return line. When the pressure becomes greater than that set by the solenoid current, the valve opens, connection is established between the primary and secondary ports and the oil flows to the tank. By changing the current in the solenoid, the pressure in the loading cylinder can be controlled and made to change accordingly.

The entire facility is controlled via the electrical panel which contains a Human Machine Interface (HMI) display. It controls both the DC valves as well as the solenoid current in the PPRV. Predefined loading signals such as square wave, ramp wave, triangular wave etc. and parameters such as cycle time, amplitude can be input.

During operation, the temperature of the oil can reach high levels which can damage the seal and other components thus causing internal contamination. The chemical and physical properties of the oil can also change in high temperatures. To prevent this, an air cooler system is present in the return line. The air cooler system contains a fan and a radiator which help cool the oil before it enters the reservoir.

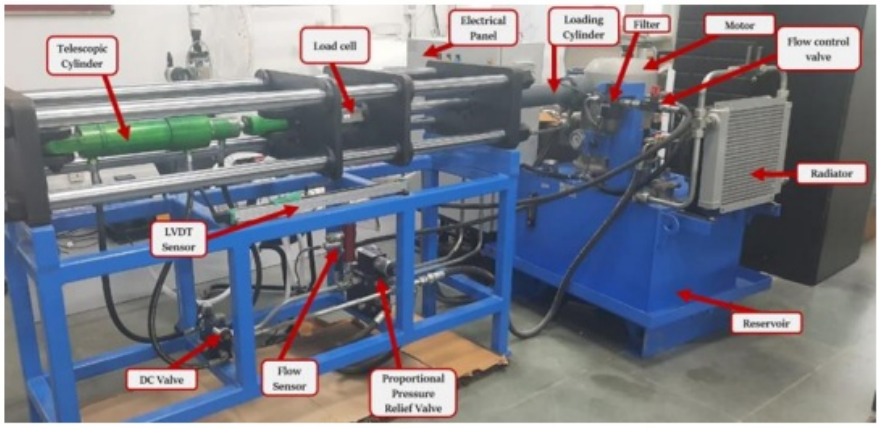

Fig 3.1: Hydraulic telescopic cylinder experimental test facility

3.4 Data Acquisition

The data is acquired using a HYDAC made Data Acquisition (DAQ) System (HMG 4000) which is an 8-channel portable data recorder. Five signals are taken as input where two pressure signals are taken from the two chambers of telescopic cylinder, two pressure signals are taken from the two chambers of hydraulic cylinder, and a total flow rate signal. The pressure sensors used are electronically compensated pressure transmitters that can measure a maximum of 600 bars. They provide a 4-20 mA output and have a operating temperature of -40°C to 100°C. These pressure sensors are connected to the portable data recorder via cables. The acquired data can then be conveniently transferred to the computer for subsequent processing as and when required. The pressure signals are input at a sampling rate of

10 kHz. The signals are taken for a full extraction-retraction cycle of the telescopic cylinder. For our study, we have set the loading signal as a ramp wave with 200 bar peak pressure and 0.1 seconds cycle time.

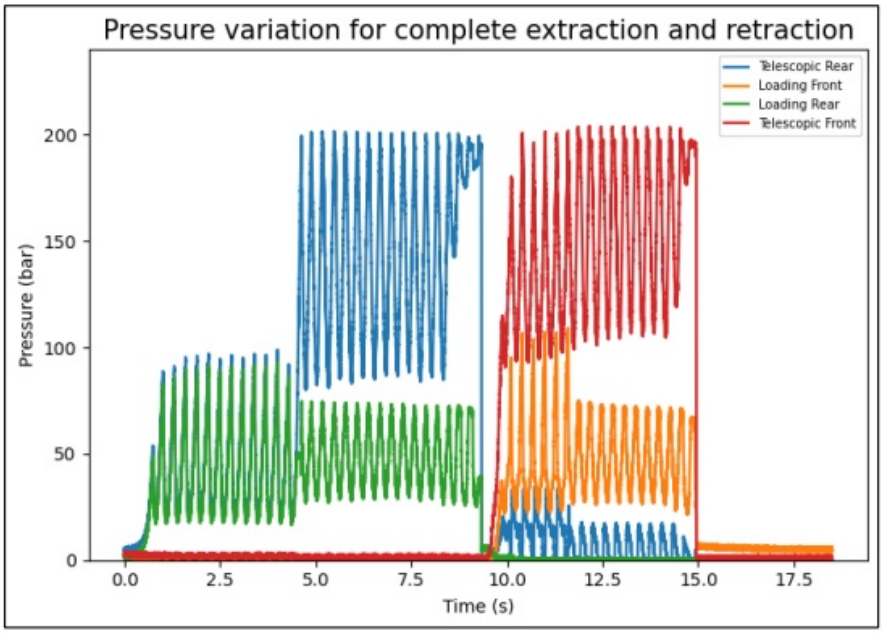

Fig 3.2: Pressure variation in both chambers of telescopic and loading cylinders

Fig 3.2 shows the variation of pressure in the telescopic cylinder and the loading cylinder in both its rear and front chamber when the seal is healthy i.e., no leakage takes place. The graph can be subdivided into two distinct segments: the extraction part and the retraction part. The extraction process occurs between 0 and 9.5 seconds, whereas the retraction process occurs between 9.5 and 15 seconds. To better understand the signals, we explore them one by one.

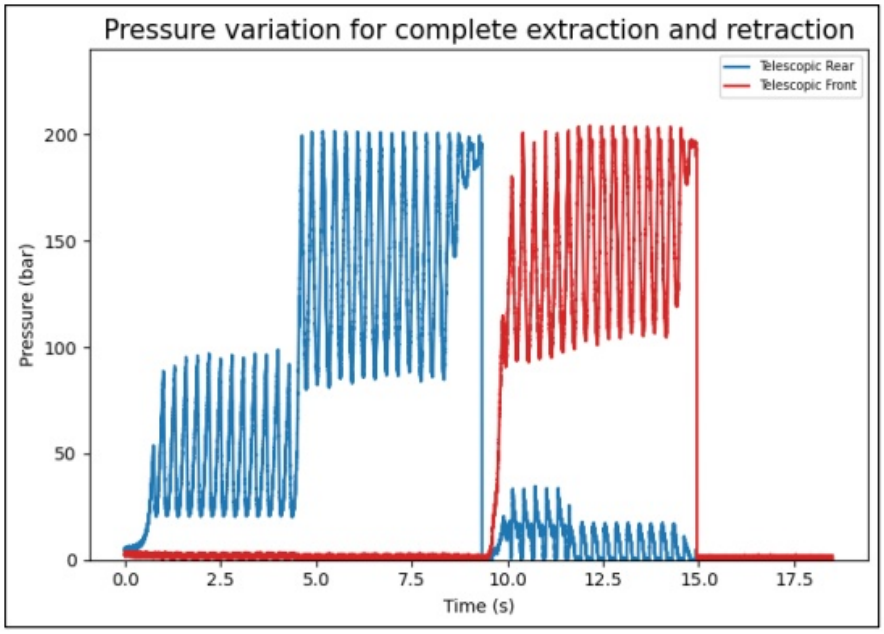

Fig 3.3: Pressure variation in both chambers of telescopic cylinder

Fig 3.3 shows the variation of pressure in both the chambers of the telescopic cylinder for one complete cycle of extraction and retraction of the telescopic cylinder. During extraction process, oil starts filling in the rear chamber of the telescopic cylinder and hence the pressure starts building up. We see that pressure initially varies approximately between 20 bars and 95 bars, and then the pressure rises and starts varying approximately between 90 bars and 200 bars. This rise in the pressure can be explained by the fact that initially the pressure of the oil is acting on the combined cross-section of the 1st stage piston and 2nd stage piston and thus less pressure is needed to overcome the resisting force by the loading cylinder as pressure times area equals force. After the 1st stage of the telescopic cylinder has fully extracted, the pressure now acts only on the cross-section of the 2nd piston due to which higher pressure is needed to overcome the resisting force. The cycle of the loading signal is 0.1 seconds i.e., pressure builds up in the loading cylinder and hence the telescopic cylinder for 0.1 seconds and then drops before again rising. Near the end of

the extraction of the second stage of telescopic cylinder, we see that the lower limit of variation in pressure starts increasing even before the full extraction has taken place. This is because of an inbuilt and pre-coded feedback mechanism which uses LVDT sensor to sense the position of the telescopic cylinder. Similarly, during retraction, we see that pressure initially varies between 80 bar and 180 bar and then rises and varies between 100 bar and 200 bar. This is again because the pressure is initially acting on a larger area and once the 1st stage cylinder has fully retracted, the area of cross-section on which the pressure of oil acts reduces thereby needing a higher pressure to overcome the resisting force.

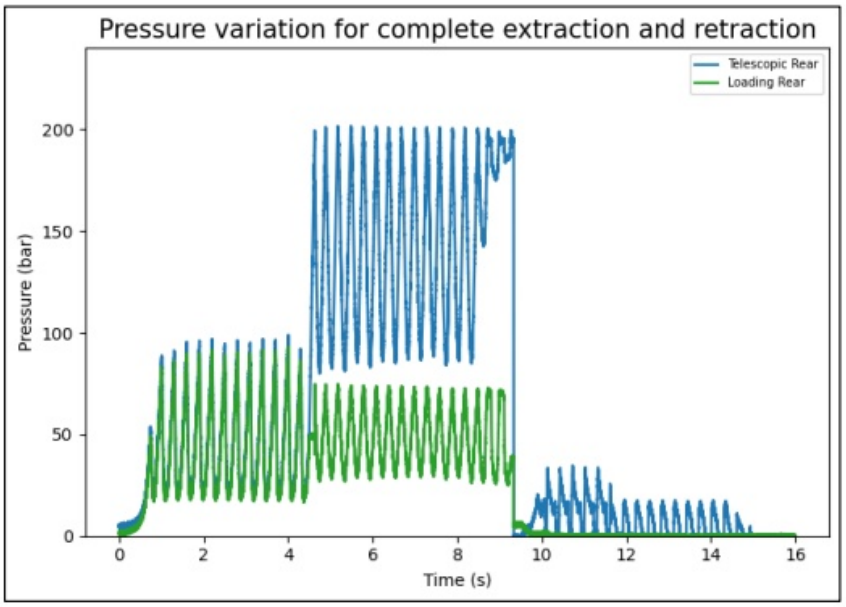

Fig 3.4: Pressure variation in the rear chambers of telescopic cylinder and loading cylinder

Fig 3.4 shows the pressure variation in the rear chambers of loading and telescopic cylinder for one complete cycle of extraction and retraction. We see that initially during the extraction of the 1st stage of the telescopic cylinder, the pressure in the rear chambers of both the cylinders are almost equal at each moment of time. This is because the cross-section area of the

piston in the loading cylinder is equal to the combined area of cross-section of both the pistons in the telescopic cylinder. Since the area is equal, the pressure also becomes equal. Once the first stage of the telescopic cylinder has fully extracted, the area of cross-section on which the oil pressure is acting reduces and hence the pressure required to overcome the resisting forces increases. The amplitude of the variation in pressure in the loading cylinder decreases. The ratio of the pressure in the telescopic cylinder to the pressure in the loading cylinder should be equal to the ratio of the area of cross-section in the loading cylinder to the area of cross-section in the telescopic cylinder.

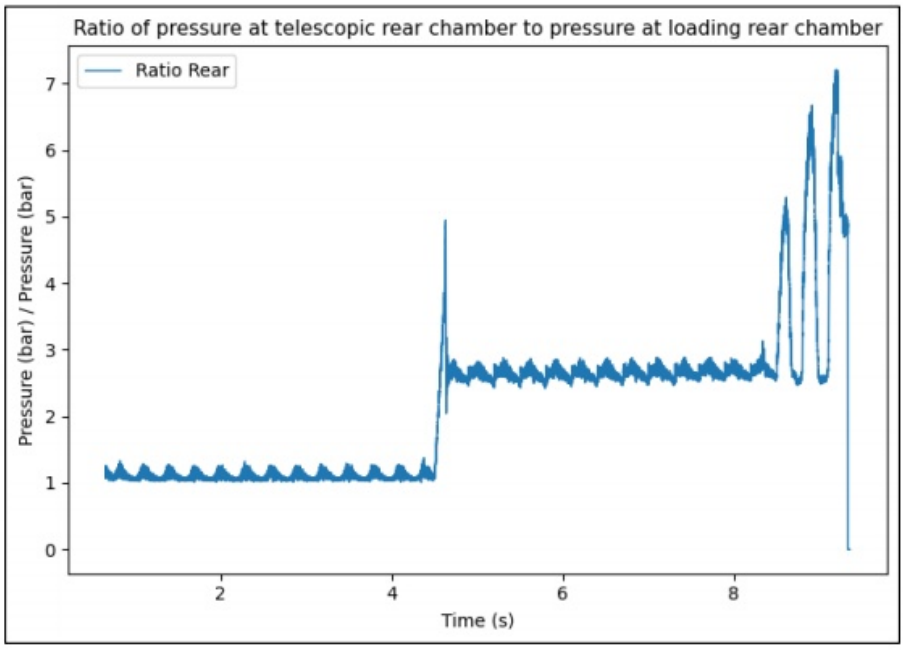

Fig 3.5: Ratio of pressure in rear chamber of telescopic cylinder to pressure in rear chamber of loading cylinder

Fig 3.5 shows the variation in ratio of pressure at telescopic rear chamber to pressure at loading rear chamber. During the extraction of 1st stage of telescopic cylinder, the ratio varies approximately from 1.09 to 1.16 and during the extraction of the 2nd stage of telescopic cylinder, the ratio varies

approximately from 2.8 to 2.97. Ideally, the ratio should be equal to the inverse ratio of cross-section areas of the pistons of the two cylinders. The area of cross-section of the piston of loading cylinder ($A_{l,r}$) is equal to $\frac{\Pi(80)^2}{4}$ mm^2. During the extraction of 1st stage of telescopic cylinder, the oil pressure is acting on the combined area of the 1st stage piston and 2nd stage piston and is equal to $\frac{\Pi(80)^2}{4}$ mm^2. After the 1st stage of telescopic cylinder has fully extracted, the pressure acts only on the 2nd piston and thus the area of cross-section ($A_{t,r}$) is equal to $\frac{\Pi(50)^2}{4}$ mm^2.

Thus, we have,

$$\left(\frac{A_{l,r}}{A_{t,r}}\right)_{stage\ I} = 1 \text{ and } \left(\frac{A_{l,r}}{A_{t,r}}\right)_{stage\ II} = 2.56$$

Since, the force exerted from both sides must be equal and force is equal to pressure times area, we have,

$$p_{t,r}A_{t,r} = p_{l,r}A_{l,r}$$

or,

$$\frac{p_{t,r}}{p_{l,r}} = \frac{A_{l,r}}{A_{t,r}}$$

Thus, ideally, we should have the ratio as follows,

$$\left(\frac{p_{l,r}}{p_{t,r}}\right)_{stage\ I} = 1 \text{ and } \left(\frac{p_{l,r}}{p_{t,r}}\right)_{stage\ II} = 2.56$$

But experimentally we get a higher ratio. If we let $\left(\frac{p_{t,r}}{p_{l,r}}\right) = k\left(\frac{A_{l,r}}{A_{t,r}}\right)$, then in both stages, k varies from 1.09-1.16.

This higher k value could be because of the mass times acceleration term which was not taken into account, or a slight delay in response of the pressure in the telescopic cylinder to the change in pressure in the loading cylinder.

Chapter 4: Internal leakage detection and classification

4.1 Introduction

Condition-based monitoring techniques are essential to monitor the health of a telescopic cylinder in real time and alert the operator in case any internal leakage fault develops. This requires monitoring change in one or more parameters of the hydraulic system to detect internal leakage.

In this study, leakage is introduced internally in the telescopic cylinder by wearing the seal. The effect of increasing seal wear on pressure signal from telescopic cylinder is studied. Various statistical time-domain features are calculated from the pressure signal to capture various aspects of the data. Four machine learning classifiers are trained to detect and characterize internal leakage of different severities.

4.2 Effect of increasing seal wear

The pressure sensor data is collected to examine three distinct levels of leakage severity. These severities are categorized as follows: a) No leakage b) Slight leakage c) Moderate leakage. To introduce these varied levels of leakage, the piston seals are ground to different lengths. For our study, the piston seal of the 1st stage piston of the telescopic cylinder is ground. A grind of 1.6 mm i.e., 2% of nominal diameter (80 mm) on the piston seal simulates slight leakage whereas a grind of 2.4 mm i.e., 3% of nominal diameter on the piston seal simulates moderate leakage condition. Thus, by replacing the piston seals on the 1st stage piston of the telescopic cylinder, we simulate different leakage conditions.

Fig 4.1 (a): Piston seal with guide rings (b) Real view of piston and seal

Fig 4.1.a shows the picture of the seal along with guide seals. Fig 4.1.b shows the seal on the 1st stage piston of the telescopic cylinder. The seal in the middle with the grooves is the piston seal to which we introduce wears. The wear was introduced in increments of 0.8 mm through a table-top grinding wheel. Change in the pressure signals was seen from 1.6 mm wear onwards. At a wear of 3.2 mm, there was severe leakage in the telescopic cylinder where the cylinder was able to extract but unable to retract.

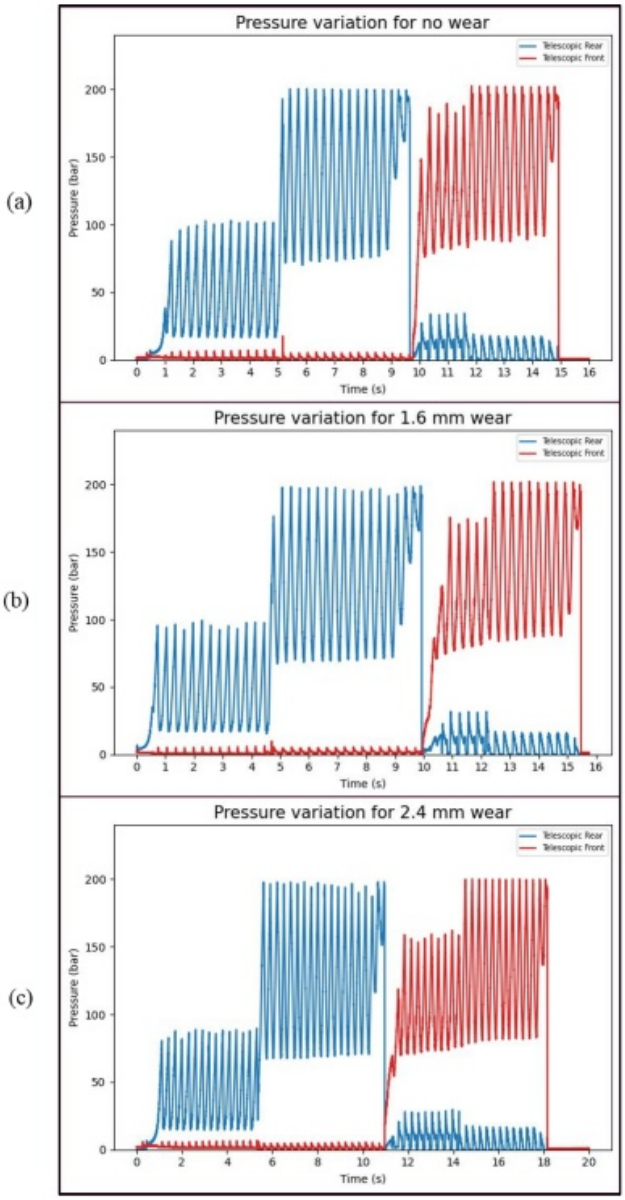

Fig 4.2: (a) Pressure variation in telescopic cylinder for no wear condition; (b) Pressure variation in telescopic cylinder for 1.6 mm seal wear; (c) Pressure variation in telescopic cylinder for 2.4 mm seal wear;

Figure 4.2 shows the variation of pressure signal with increasing wear. For no wear condition i.e., no leakage, the variation in pressure in the telescopic rear and telescopic front chamber is shown in Fig 4.2.a. As the wear

increases to 1.6 mm (2% of nominal diameter), a slight drop in pressure values is seen in both the chambers. In the telescopic rear chamber, a pressure drop of 2-3 bar is observed during the extraction of the 1st stage and the 2nd stage of the telescopic cylinder. At 2.4 mm wear (3% of nominal diameter), a significant pressure drop is observed in both the telescopic rear and telescopic front chamber during the extraction and retraction of 1st stage of the telescopic cylinder respectively. During the extraction of the 1st stage of the telescopic cylinder, a pressure drop of 10 bar is observed in the telescopic rear chamber whereas during retraction, a pressure drop of 20 bar is observed in the telescopic front chamber. This is because as the wear is increased, the leakage between the telescopic rear and telescopic front chamber increases, and the rate of pressure build up in the chambers decreases. As the cycle time of loading signal is 0.1 seconds, the pressure is not able to reach its no wear levels in time due to decreased pressure build up rate and thus results in a pressure drop. The total time taken for completing one cycle of extraction and retraction also increases as the seal wear increases. For no wear level, the cycle is completed in approximately 15 seconds. For 1.6 mm wear level, the cycle completion time slightly increases to 15.3-15.4 seconds and for 2.4 mm wear level, the cycle completion time increases to around 18 seconds i.e., 3 seconds more than that for no wear level.

4.3 Workflow

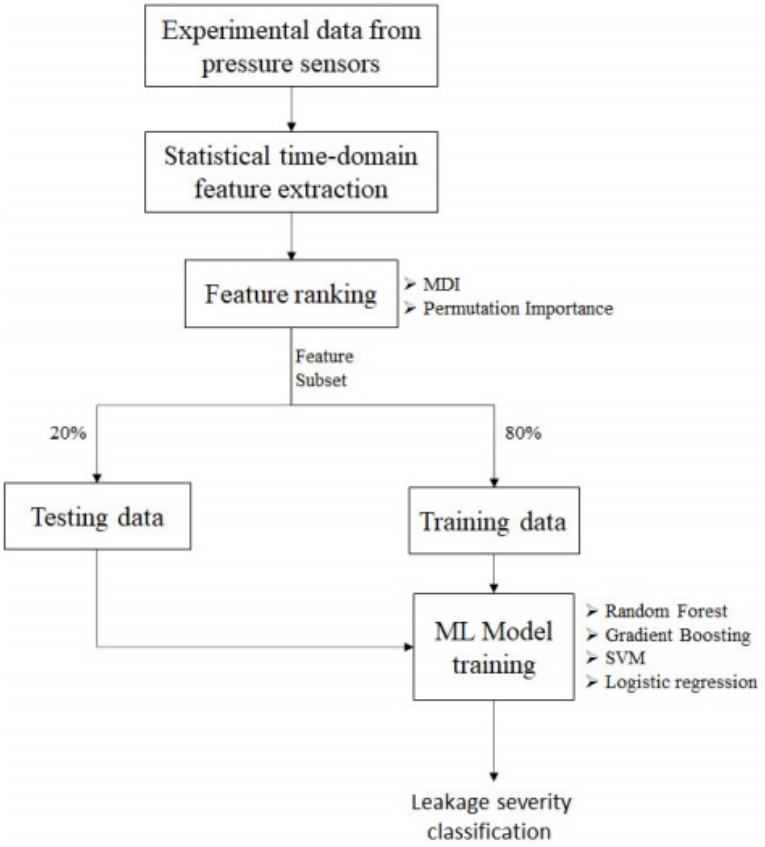

Fig 4.3: Flowchart for internal leakage detection and classification

Fig 4.3 shows the procedure followed for internal leakage detection and classification based on four machine learning classification algorithms. Pressure data is gathered from the experimental test facility for three different leakage severities: no leakage (0 mm wear), slight leakage (1.6 mm wear), and moderate leakage (2.4 mm wear). Statistical time domain features are calculated from the pressure data. Feature ranking methods are used to obtain the eight most relevant features. A dataset is created with these features and is divided into two parts: training data and testing data in the ration 8:2. The training data is used to train 4 different machine learning

based classifiers and its accuracy is checked on the testing data for detection and classification of leakage severity.

4.4 Statistical time-domain feature extraction

To analyze and gain insight from the pressure signals, we can extract several statistical features from the signal. Statistical features provide and summarize valuable information about the signal, and a greater understanding of its characteristics and behavior. Further, they help analyze the distribution of data such as the central tendency, outliers, and overall variability of the signal.

Therefore, as a preliminary step, we extract the following nine distinct statistical time-domain features from each pressure signal:

i. **Mean:** Mean is a measure of central tendency that represents the arithmetic average of all the values in the signals. It indicates the average level of the signal and is commonly used as a basic statistical descriptor to understand the overall magnitude or baseline of a signal. Mathematically, it is defined as follows:

$$\bar{x} = \frac{\sum_{i=1}^{n} x_i}{n}$$

ii. **Standard deviation (σ):** The standard deviation of a signal is a measure of the dispersion or variability of the values in the signal. It quantifies how much the values deviate from the mean of the signal. The mathematical formula for standard deviation is as follows:

$$\sigma = \sqrt{\frac{\sum_{i=1}^{n}(x_i - \bar{x})^2}{n}}$$

iii. **Root mean square (RMS):** The root mean square (RMS) value of a signal provides information about the overall magnitude or amplitude of the signal. The RMS value is calculated by taking the square root of the mean of the squared values of the pressure signal. The RMS value is useful in quantifying the effective power or energy contained in the signal. It is defined mathematically as below:

$$RMS = \sqrt{\frac{\sum_{i=1}^{n} x_i^2}{n}}$$

iv. **Kurtosis:** The kurtosis of a signal describes the peakedness of the probability distribution of the signal's values. It quantifies the extent to which the distribution of the signal deviates from a normal distribution and provides information about the tails of the distribution and whether they are heavier or lighter than those of a normal distribution. Positive kurtosis indicates that a signal has heavier tales and a sharper peak while a negative kurtosis indicates that a signal has lighter tales and a flatter peak. Its mathematical formula is given below:

$$Kurtosis = \frac{\frac{1}{n}\left(\sum_{i=1}^{n}(x_i - \bar{x})^4\right)}{\sigma^4}$$

v. **Skewness:** Skewness of a signal quantifies the asymmetry of the signal's distribution around its mean. It indicates whether the tail of the distribution leans towards the left (negative skewness) or to the right (positive skewness). A skewness value of 0 indicates a perfectly symmetric distribution. Skewness can be calculated mathematically by the following formula:

$$Skewness = \frac{\frac{1}{n}\left(\sum_{i=1}^{n}(x_i - \bar{x})^3\right)}{\sigma^3}$$

vi. **Crest Factor:** The crest factor of a signal is a measure of the peak-to-average amplitude ratio. It quantifies the extent of peak values in relation to the average or RMS value of the signal. A higher crest factor indicates a signal with larger peak values compared to its average or RMS value, indicating a more "peaky" or "spiky" waveform whereas a lower crest factor indicates a signal with a relatively smaller difference between the peak and average or RMS values, suggesting a "smoother" or "uniform" waveform. The mathematical formula for crest factor is as follows:

$$Crest\ Factor = \frac{Peak\ value}{RMS\ value}$$

vii. **Clearance factor:** Clearance factor of a signal is mathematically defined as the absolute peak value of the signal divided by the squared mean value of the square roots of the absolute values of amplitudes. The mathematical formula for clearance factor is as follows:

$$Clearance\ factor = \frac{max(|x_i|)}{\left(\frac{\sum_{i=1}^{n}\sqrt{|x_i|}}{n}\right)^2}$$

viii. **Shape factor:** Shape factor is defined as the ratio of the root mean square to mean of absolute value of the signal. It provides information about a signal's shape i.e., whether is more peaky or more rounded. The mathematical formula for shape factor is as follows:

$$Shape\ Factor = \frac{RMS\ value}{Average\ absolute\ value}$$

ix. **Impulse factor:** The impulse factor of a signal is a measure of its peak amplitude relative to its energy content. A higher impulse factor indicates that the signal has a sharper or more impulsive shape, with a larger peak amplitude relative to its energy. On the other hand, a lower impulse factor suggests a more spread out or less impulsive signal. The mathematical formula for impulse factor is as follows:

$$Impulse\ Factor = \frac{Peak\ value}{Average\ absolute\ value}$$

4.5 Feature selection

Statistical features can be used to identify the most relevant and informative aspects of the signal. This aids in decreasing the dimensionality of the data and determining the most important features for further analysis or modeling. There are various common types of feature selection methods used in machine learning and data analysis. They can be segregated into three main categories: a) filter methods; b) wrapper methods; and c) embedded methods. Feature selection is carried out by embedded models as part of the model training process to optimize both feature selection and model parameters simultaneously. Embedded methods are usually more robust, efficient and tend to produce more generalizable feature subsets compared to the other two types of methods. Tree-based methods fall in this category. Tree-based models like Decision Trees (DT), Random Forests (RF) and Gradient Boosting Machines have built-in feature importance measures that rank the features based on their contribution to the model's predictive performance.

4.5.1 Feature ranking using MDI method

The feature importance in Random Forest is typically computed based on the collective behavior of the decision trees in the ensemble. Random Forest calculates feature importance by considering how much each feature decreases the impurity or randomness in the forest's predictions. When a decision tree splits the data based on a feature, it evaluates the improvement in impurity achieved by that split. The feature importance is then determined by averaging the impurity reduction across all trees in the Random Forest. The feature importance values are typically normalized to sum up to 1. Features that consistently lead to a significant reduction in impurity across the ensemble are considered more important. Higher values indicate a stronger contribution of a feature to the model's predictive performance. The feature importance values can be used to rank the features in descending order, where the most important features have higher values. Thus, features are ranked based on mean decrease in impurity (MDI).

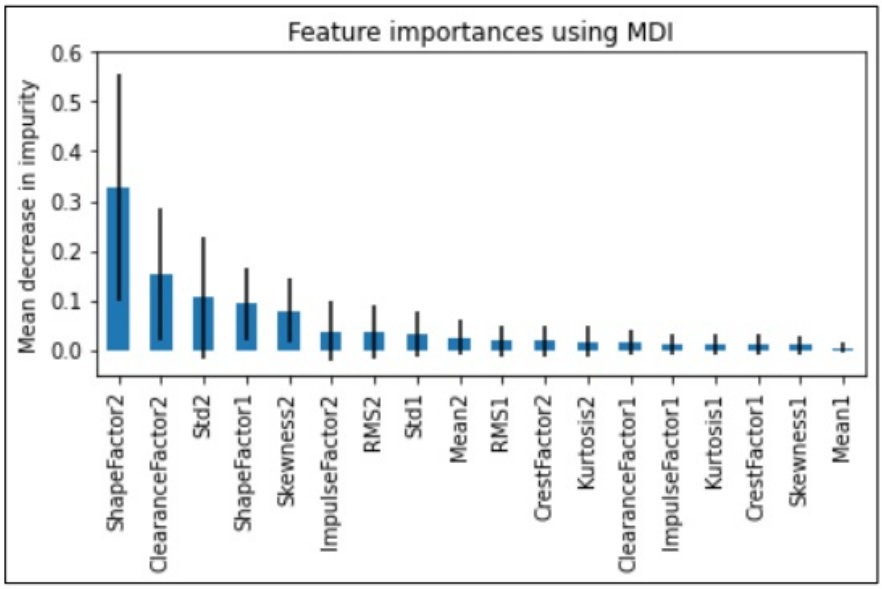

Fig 4.4: Feature importances using MDI

Fig 4.4 shows the various features in descending order of mean decrease in impurity. The number '1' and '2' at the end of the features indicate that the features have been calculated using the pressure signals in the rear and front chamber of the telescopic cylinder respectively. From this graph, it is clear that the features extracted from the pressure signal from the front chamber of the telescopic cylinder have much more significant than those extracted from the rear chamber of the telescopic cylinder.

4.5.2 Feature ranking using permutation feature importance

Permutation feature importance is another method used to evaluate the importance of each feature in a machine learning model. It measures the impact of shuffling or permuting the values of a feature on the model's performance thereby breaking their relationship with the target variable. By evaluating the change in model performance when a feature's values are randomly permuted and comparing it to pre-permutation performance, we can determine the importance of that feature in making accurate predictions. This is repeated for each feature in the dataset, independently shuffling and evaluating their performance. The importance scores are then ranked to identify the most important features.

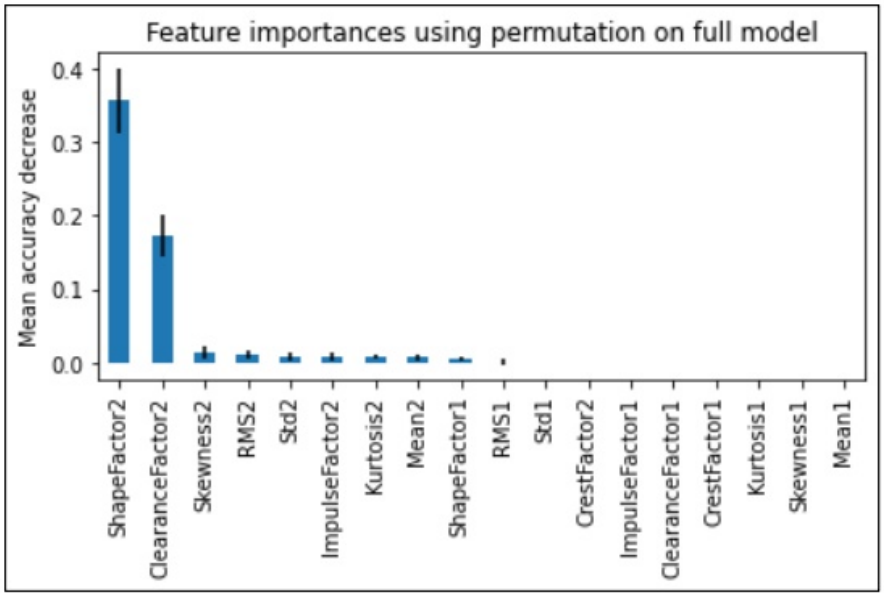

Fig 4.5: Feature importances using permutation on full model

Figure 4.5 demonstrates that both methods identify the same set of features as being of utmost importance, albeit with varying degrees of relative importance. Furthermore, it is observed that the MDI method exhibits a higher tendency to retain all features, unlike permutation importance which has a higher likelihood of excluding certain features entirely.

ML models are trained using the 8 most important features as identified in Fig 4.5, namely, ShapeFactor2, ClearanceFactor2, Skewness2, RMS2, Std2, ImpulseFactor2, Kurtosis2 and Mean2.

4.6 Scatterplot matrix

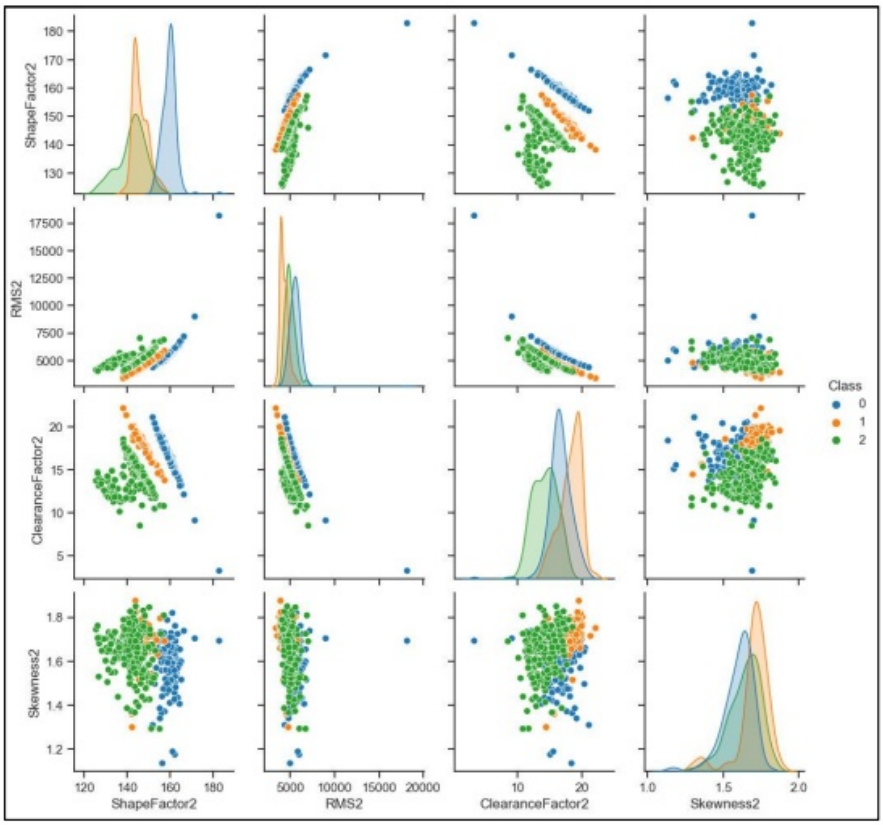

Fig 4.6: Scatterplot matrix of top 4 ranked features

Fig 4.6 shows the scatter plot matrix of the four most important features as ranked by the feature ranking methods, namely, ShapeFactor2, ClearanceFactor2, RMS2, Skewness2. On the diagonal elements of the matrix, we see the distribution of the features. Most of the features follow the normal distribution. On the non-diagonal elements of the matrix, we see that the scatter plot of the feature against other features. The data in blue colour in the above scatter plots indicates the no wear data, the data in orange colour indicates the 1.6 mm wear data and the data in green colour indicates the 2.4 mm wear data. From the scatter plots, we see that the data for moderate leakage forms larger and more spread-out clusters unlike the close clusters formed by data for slight leakage and no leakage. Further,

there is significant overlap between the clusters which makes the classification based simply on these features hard. From the scatter plots, information about correlation between different features can also be extracted. The features ShapeFactor2 and ClearanceFactor2 are negatively correlated while ShapeFactor2 and RMS2 are positively correlated. For other features, there is no clear correlation between them. For better and more accurate classification based on these features, four machine learning models have been trained on the data and comparison has been done between their accuracies.

4.7 Machine Learning Models

Four machine learning models have been used in this study to predict and classify the severity of leakage in the telescopic cylinder. A comparison between their accuracies has been done.

4.7.1 Random Forest

Random Forest is an ensemble learning method that combines multiple decision trees to make predictions. It belongs to the family of tree-based models and is an extension of the decision tree algorithm. However, unlike a single decision tree, which can be prone to overfitting, Random Forest mitigates overfitting and provides better generalization by introducing randomness into the model.

The Random Forest algorithm works by creating an ensemble of decision trees. Each tree in the forest is trained on a randomly sampled subset of the training data (known as bootstrapping) and uses a random subset of features for each split. These randomization procedures introduce diversity among the trees, reducing their correlation. To make predictions, it aggregates the predictions of all individual trees and the class with the majority vote among

the trees is selected. Random Forest model is resistant to overfitting due to the randomness introduced in the sampling and feature selection processes. It can handle high-dimensional data and large datasets effectively and requires little data pre-processing.

4.7.2 Gradient Boosting

Gradient Boosting is an ensemble learning method. It creates a strong predictive model by combining together relatively weak predictive models. The key idea behind Gradient Boosting is to iteratively build a sequence of models, each one focusing on correcting the mistakes made by the previous models. An initial model, typically a decision tree, is created first which serves as the starting point of the algorithm. This model is then used to make predictions on the training data. The differences between the predicted values and the actual target values are calculated. These differences represent the residuals or errors of the initial model. These residuals then become the new target values for the subsequent model to predict. In this way each new model is trained to reduce and minimize the error of the previous model by fitting the negative gradient of the loss function. In this study, the log loss function has been used as the loss function for gradient boosting algorithm. To get the final prediction, the predictions from all the weak learners are combined by summing the predictions of all the models, weighted by a learning rate that controls the contribution of each model. The learning rate acts as a regularization parameter, preventing overfitting and allowing better generalization.

4.7.3 Logistic Regression

Logistic Regression is a type of generalized linear model that predicts the probability of an observation belonging to either of two classes or outcomes typically represented by 0 and 1. It estimates the probability of the

dependent variable being in the positive class (1) given the values of the independent variables. The Logistic Regression model uses the sigmoid function to map the linear combination of the independent variables to a probability value between 0 and 1. Thus logistic regression inherently performs binary classification. It can be extended to perform multi-class classification using the "One-vs-Rest" approach where a separate logistic regression model is trained for each class, considering it as the positive class and the rest of the classes as the negative class. This results in as many logistic regression models as the number of classes, each producing a probability estimate for its respective class. During prediction, the class with the highest probability is selected as the predicted class.

4.7.4 Support Vector Machine (SVM)

SVM is a supervised machine learning model that aims to find an optimal hyperplane that best separates the data points of different classes in the feature space. The hyperplane is calculated in a way that maximizes the margin. Margin is the distance between the hyperplane and the closest data points from each class. Those data points that are closest to the hyperplane are called support vectors. Support vector machines can handle both linearly separable and non-linearly separable data by using a technique called the kernel trick. The kernel trick allows SVM model to transform the original feature space into a higher-dimensional feature space, where the data may become linearly separable. In this study, we use the quadratic kernel.

4.8 Comparison of performance of machine learning models

The machine learning models were trained on the eight most important features as identified by the feature ranking by permutation method. 10-fold cross-validation was implemented on the training data to prevent overfitting. The performance of classification machine learning models is

studied using evaluation metrics such as accuracy, confusion matrix, precision and recall etc. A confusion matrix provides a detailed breakdown of the model's predictions for each class. It shows the number of true positives, true negatives, false positives, and false negatives. From the confusion matrix, other metrics such as precision, recall, and F1 score can be derived.

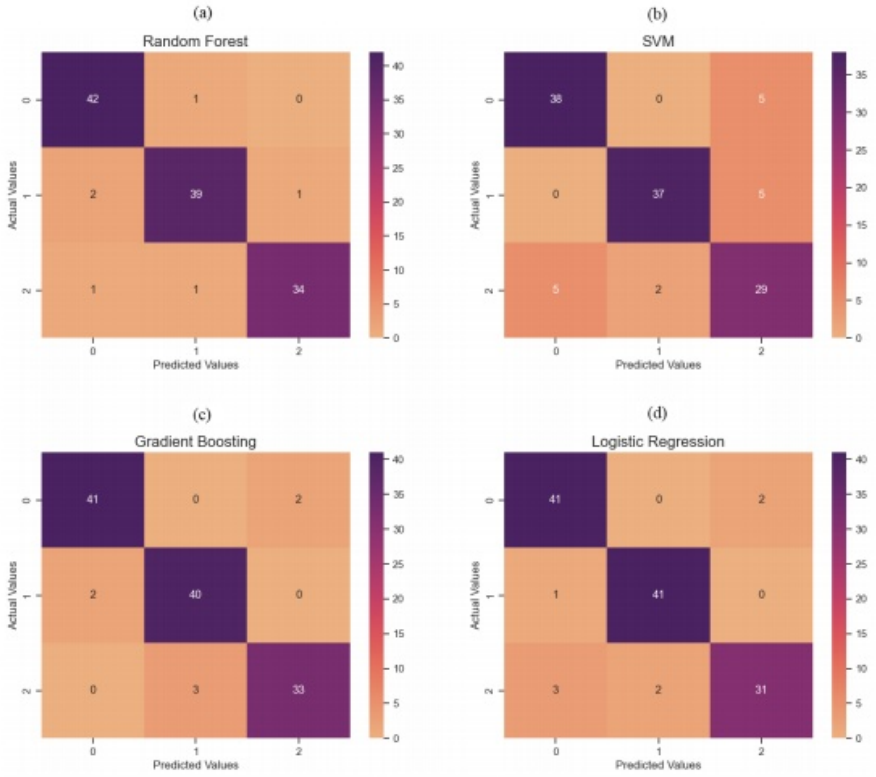

Fig 4.7: Confusion matrices for Random Forest, SVM, Gradient Boosting and Logistic Regression classifiers

Fig 4.7 shows the confusion matrices for the four machine learning algorithms. The number on the i^{th} row and j^{th} column of a confusion matrix represents the number of observations which belonged to class i but was predicted by the model to belong to class j. Thus, numbers on the diagonals represent the number of correct classifications while the non-diagonal

numbers represent the incorrect predictions by the model. From Fig 4.7, it was observed that Random Forest had the highest number of correct predictions followed by Gradient Boosting. SVM had the highest number of mis-classifications.

Table 4.1: Comparison of test and cross-validation accuracies for four machine learning classifiers

ML Model	Test Accuracy (%)	Cross-validation accuracy (%)
Gradient Boosting	94.21	96.51
SVM	85.95	90.43
Random Forest	95.04	95.78
Logistic Regression	93.38	97.36

Accuracy is a popular evaluation metric that gives a measure of the overall correctness of the model's predictions. It is calculated by dividing the number of correct predictions by total number of predictions. We can derive it from the confusion matrix as the sum of the diagonal elements divided by total number of elements in the matrix. Table 4.1 shows the test accuracy and cross validation accuracy of the various machine learning models. We see that Random Forest was most accurate in predicting the severity of leakage with an accuracy of 95.04%. The SVM algorithm had the lowest accuracy of 85.95%. This could be because of the inherent nature of SVM algorithm which makes it very good for binary classification but not for multi-class classification. In general, tree-based classifiers such as Gradient Boosting and Random Forest performed better than non-tree-based classifiers.

Chapter 5: Conclusion and Scope for future work

5.1 Conclusion

In this study, four classification-based methods for condition monitoring of hydraulic telescopic cylinders to detect fluid leakage of two different severities (2% and 3% of nominal diameter) were developed. A high pressure (210 bar) hydraulic telescopic cylinder test rig was used to study and simulate the effect of internal fluid leakage in a two-stage telescopic cylinder. The pressure signals from the two chambers of telescopic cylinder were studied and it was seen that pressure values were lower during extraction or retraction of the 1st stage of telescopic cylinder than that during the extraction or retraction of 2nd stage. The relation between the pressure signals from the loading cylinder and the pressure signals from the telescopic cylinder was explored where it was seen that the signals vary such that the ratio of pressure in the cylinders is equal to the inverse ratio of their areas of cross-section on which the fluid pressure is acting. The effect of increasing wear on the pressure signals was observed that as the seal wear increased there was a pressure drop in the signals and the time for extraction and retraction increased. Statistical time domain features were extracted from the pressure signals and feature ranking methods were applied to identify the most relevant features for detecting internal fluid leakage in the cylinder. Shape factor of the pressure signals from the front chamber of telescopic cylinder was identified as the most relevant feature. Four classifiers were trained on these features to detect and identify the severity of internal leakage. The accuracy of the random forest classifier was the highest with 95.04% accuracy followed by gradient boosting, logistic regression and SVM. The SVM-based classifier had the lowest accuracy with 85.95% accuracy. Leakage was detected using only the pressure signals from the two chambers of the telescopic cylinder.

5.2 Future scope

The results of the study highlight that internal leakage can be detected in telescopic cylinders with good accuracy (95%) using only the pressure signals from the two chambers of the telescopic cylinder with little data preprocessing. This has good potential for use in industry as it can reduce the cost and complexity of the monitoring framework. Using online condition monitoring, severity of internal leakage can be identified in telescopic cylinders in real time and accordingly maintenance can be scheduled before the severity increases further.

Future studies can focus on frequency domain analysis of internal leakage faults in telescopic cylinders and effect of different loading conditions on leakage severity. Further, the current study can be extended to estimate the remaining useful life (RUL) of the seal.

References

[1] Commercial Hydraulics. Designing With Cylinders Telescopic Cylinders. Parker Hannifin Corporation, Mobile Cylinder Division, Youngstown, OH

[2] Power & Motion (2006), Telescoping cylinders go the extra distance. Accessed on: 24th May, 2023. Available on: https://www.powermotiontech.com/technologies/cylinders-actuators/article/21884652/telescoping-cylinders-go-the-extra-distance

[3] Johny, Cherian & Sivadas, K.R. (2016), Case Study and Critical analysis to find the FMEA in Hydraulics System. ICETEM'16

[4] X. Wu, Y. Li, F. Li, Z. Yang and W. Teng (2012), Adaptive Estimation-Based Leakage Detection for a Wind Turbine Hydraulic Pitching System, in *IEEE/ASME Transactions on Mechatronics*, vol. 17, no. 5, pp. 907-914, doi: 10.1109/TMECH.2011.2142400.

[5] R. G. McQueen and W. Boyes, Fluid Power Seals and Sealing Technology. In: R. G. McQueen (ed.), Fluid Power Engineering, chapter 6. Butterworth-Heinemann, 2009.

[6] Prasanna S. Mahankar, Ashwinkumar S. Dhoble (2021), Review of hydraulic seal failures due to effect of medium to high temperature, Engineering Failure Analysis, Volume 127, 105552, ISSN 1350-6307, https://doi.org/10.1016/j.engfailanal.2021.105552.

[7] Y. Miao and S. Wang (2011), Failure diagnosis of hydraulic lifting system based on multistage telescopic cylinder, Proceedings of 2011 International Conference on Fluid Power and Mechatronics, Beijing, China, 2011, pp. 828-834, doi: 10.1109/FPM.2011.6045876.

[8] V. V Shanbhag, T. J. J. Meyer, L. W. Caspers, and R. Schlanbusch (2020), Diagnostics of seal and rod degradation in hydraulic cylinders using acoustic emissions, in Proc. Eur. Conf. PHM Soc., pp. 1–8. Available: http://www.phmpapers.org/index.php/phme/article/view/1173

[9] S. J. Shen and Q. H. Yang (2011), Analysis and solution of hydraulic cylinder's leakage problem, Adv. Mater. Res., vol. 189–193, pp. 664–667, doi: 10.4028/www.scientific.net/AMR.189-193.664

[10] Puqing Luo,Jianzhong Hu,Shijun Tan (2017). Design and Realization of Hydraulic Cylinder. Region - Water Conservancy, Yueyang University of Technology, Hunan, China.

[11] C. Gonzalez (2017), 7 common failures of hydraulic seals, Mach. Des.

[12] P.J. Gamez-Montero, E. Salazar, R. Castilla, J. Freire, M. Khamashta, E. Codina (2009), Misalignment effects on the load capacity of a hydraulic cylinder, International Journal of Mechanical Sciences, Volume 51, Issue 2, Pages 105-113, ISSN 0020-7403, https://doi.org/10.1016/j.ijmecsci.2009.01.001.

[13] Noria Corporation (2001), Water in oil contamination, Machinery Lubrication. Accessed: May 24, 2023. Available: https://www.machinerylubrication.com/Read/192/water-contaminant-oil

[14] Y. Du, T. Wu, and R. Gong (2017), Properties of water-contaminated lubricating oil: Variation with temperature and small water content, Tribol.—Mater. Surf. Interfaces, vol. 11, pp. 1–6, doi: 10.1080/17515831.2017.1279845.

[15] B. Battat and W. Babcock (2006), Reducing the effects of contamination on hydraulic fluids and systems, Pract. Oil Anal., 2006. Accessed: May 24, 2023. Available: https://www.machinerylubrication.com/Read/957/hydraulic-fluids-contamination

[16] Eaton (2002), The systematic approach to contamination control, 2002. Accessed: May 24, 2023. Available: https://www.eaton.com/ecm/groups/public/@pub/@eaton/@hyd/documents/content/ct_233707.pdf

[17] QuadFluidDynamics (2018), Understanding Drift in Hydraulic Cylinders. Accessed on 23rd May, 2023. Available on:

https://www.quadfluiddynamics.com/understanding-drift-in-hydraulic-cylinders

[18] Brendan Casey (2007), The Root Cause of Hydraulic Cylinder Drift. Machinery Lubrication. Accessed on: 25th May, 2023. Available on: https://www.machinerylubrication.com/Read/1119/hydraulic-cylinder-drift

[19] Web Desk (2020), Hydraulic Cylinder Drift: Major Reasons and Troubleshooting Tips. Worldwide Hydraulic Professionals. Accessed on: 25th May, 2023. Available on: https://whyps.com/hydraulic-cylinder-drift-major-reasons-and-troubleshooting-tips

[20] Brendan Casey (2016), How To Troubleshoot Hydraulic Cylinder Drift. Power & Motion. Accessed on: 25th May, 2023. Available on: https://www.powermotiontech.com/hydraulics-at-work/article/21885179/how-to-troubleshoot-hydraulic-cylinder-drift

[21] Gonzalo A. Barillas, Steven Cowell, Martin Goerres, Wolfgang Lipphardt, Uwe Siegrist, Sascha Möller, Sealing Systems for Hydraulic Cylinders. Freudenberg Sealing Technologies GmbH, Lead Center Fluidpower Industry, Germany

[22] Viriato, Nuno & Vaz, Mário & Castro, P.M.S.T.. (2016). Failure analysis of the rod of a hydraulic cylinder. Procedia Structural Integrity. 1. 173-180. 10.1016/j.prostr.2016.02.024.

[23] Atos Catalog, Cylinders Troubleshooting. Accessed on: 25th May, 2023.

[24] P. Chen, P. S. K. Chua, and G. H. Lim (2007), A study of hydraulic seal integrity, Mech. Syst. Signal Process., vol. 21, pp. 1115–1126, doi: 10.1016/j.ymssp.2005.09.002.

[25] L. Lloyd (2000), Hydraulic system leakage—The destructive drip, Machinery Lubrication, 2000. Accessed: May 22, 2023. Available: https://www.machinerylubrication.com/Read/21/hydraulic-systemleakage

[26] J. Koochaki, J. Bokhorst, H. Wortmann, and W. Klingenberg (2011), Evaluating condition based maintenance effectiveness for two processes in

series, J. Qual. Maintenance Eng., vol. 17, pp. 398–414, doi: 10.1108/13552511111180195.

[27] Greg Arbour (2019), What Are The 4 Types of Maintenance Strategies? Rockwell Automation. Available: https://www.fiixsoftware.com/blog/evaluating-maintenance-strategies-select-model-asset-management/

[28] Richard (Doc) Palmer (2012), Maintenance Planning and Scheduling Handbook. 3rd Edition, McGraw Hill Publication.

[29] J. Luo, K. R. Pattipati, L. Qiao, and S. Chigusa (2008), Model-based prognostic techniques applied to a suspension system, IEEE Trans. Syst., Man, Cybern., A, Syst. Humans, vol. 38, no. 5, pp. 1156–1168.

[30] Qingliang Zeng, Wenting Liu, Lirong Wan, Chenglong Wang, and Kuidong Gao (2020), Maintenance Strategy Based on Reliability Analysis and FMEA: A Case Study for Hydraulic Cylinders of Traditional Excavators with ERRS, Mathematical Problems in Engineering, vol. 2020, Article ID 2908568, 11 pages, https://doi.org/10.1155/2020/2908568

[31] T. Xi, S. Kehne, T. Fujita (2020), A. Epple, and C. Brecher, Condition monitoring of ball-screw drives based on frequency shift, IEEE/ASME Trans. Mechatronics, vol. 25, no. 3, pp. 1211–1219.

[32] K. Kim and A. G. Parlos (2002), Induction motor fault diagnosis based on neuropredictors and wavelet signal processing, IEEE/ASME Trans. Mechatronics, vol. 7, no. 2, pp. 201–219.

[33] Domingo Llorente Rivera, Markus R. Scholz, Michael Fritscher, Markus Krauss, Klaus Schilling (2018), Towards a Predictive Maintenance System of a Hydraulic Pump. IFAC-PapersOnLine, Vol 51, Issue 11, 2018, Pages 447-452, ISSN 2405-8963, https://doi.org/10.1016/j.ifacol.2018.08.346.

[34] S. Barber and P. Golbeck (2006), Wind turbine maintenance & condition monitoring, World Wind Energy Assoc., Bonn, Germany.

[35] Norwegian Petroleum, Investment and operating cost, 2021. Accessed: May 22, 2023. Available: https://www.norskpetroleum.no/en/economy/investments-operating-costs/

[36] E. Jantunen (2002), A summary of methods applied to tool condition monitoring in drilling, Int. J. Mach. Tools Manuf., vol. 42, pp. 997–1010, 2002, doi: 10.1016/S0890-6955(02)00040-8.

[37] K. P. Zhu, Y. S. Wong, and G. S. Hong (2009), Wavelet analysis of sensor signals for tool condition monitoring: A review and some new results, Int. J. Mach. Tools Manuf., vol. 49, pp. 537–553, doi: 10.1016/j.ijmachtools.2009.02.003.

[38] Shanbhag, Vignesh V., Thomas J. J. Meyer, Leo W. Caspers and Rune Schlanbusch (2021), Failure Monitoring and Predictive Maintenance of Hydraulic Cylinder—State-of-the-Art Review. *IEEE/ASME Transactions on Mechatronics* 26 (2021): 3087-3103.

[39] I. S. Cade, P. S. Keogh, and M. N. Sahinkaya (2005), Fault identification in rotor/magnetic bearing systems using discrete time wavelet coefficients, IEEE/ASME Trans. Mechatronics, vol. 10, no. 6, pp. 648–657, Dec. 2005.

[40] A. Yazdanpanah Goharrizi and N. Sepehri (2010), A Wavelet-Based Approach to Internal Seal Damage Diagnosis in Hydraulic Actuators, in IEEE Transactions on Industrial Electronics, vol. 57, no. 5, pp. 1755-1763, May 2010, doi: 10.1109/TIE.2009.2032198.

[41] A. Y. Goharrizi and N. Sepehri (2011), A Wavelet-Based Approach for External Leakage Detection and Isolation From Internal Leakage in Valve-Controlled Hydraulic Actuators, in *IEEE Transactions on Industrial Electronics*, vol. 58, no. 9, pp. 4374-4384, Sept. 2011, doi: 10.1109/TIE.2010.2095396.

[42] X. Zhao, S. Zhang, C. Zhou, Z. Hu, R. Li, and J. Jiang (2015), Experimental study of hydraulic cylinder leakage and fault feature extraction based on wavelet packet analysis, Comput. Fluids, vol. 106, pp. 33–40, 2015

[43] Tang, H. B., Wu, Y. X., & Ma, C. X. (2010), Inner Leakage Fault Diagnosis of Hydraulic Cylinder Using Wavelet Energy. In Advanced Materials Research (Vols. 139–141, pp. 2517 2521). Trans Tech Publications, Ltd. https://doi.org/10.4028/www.scientific.net/amr.139141.2517

[44] A. Y. Goharrizi and N. Sepehri (2012), Internal leakage detection in hydraulic actuators using empirical mode decomposition and Hilbert spectrum, IEEE Trans. Instrum. Meas., vol. 61, no. 2, pp. 368–378, Feb. 2012

[45] Li L, Huang Y, Tao J, Liu C (2019), Internal leakage identification of hydraulic cylinder based on intrinsic mode functions with random forest. Proceedings of the Institution of Mechanical Engineers, Part C: Journal of Mechanical Engineering Science. 2019;233(15):5532-5544. doi:10.1177/0954406219846148

[46] Lu C, Wang S and Zhang C (2015), Fault diagnosis of hydraulic piston pumps based on a two-step EMD method and fuzzy C-means clustering. Proc IMechE, Part C: Journal of Mechanical Engineering Science 2015; 230: 2913–2928.

[47] Rai A, Upadhyay SH (2018), Intelligent bearing performance degradation assessment and remaining useful life prediction based on self-organising map and support vector regression. Proceedings of the Institution of Mechanical Engineers, Part C: Journal of Mechanical Engineering Science. 2018;232(6):1118-1132. doi:10.1177/0954406217700180

[48] Madhumitha Ramachandran, Zahed Siddique (2019), A Data-Driven, Statistical Feature Based, Neural Network Method for Rotary Seal Prognostics. Journal of Non-destructive evaluation, diagnostics and prognostics of engineering systems, Volume 2, Issue 2 (May 2019).

[49] Mariela Cerrada, Grover Zurita, Diego Cabrera, René-Vinicio Sánchez, Mariano Artés, Chuan Li (2016), Fault diagnosis in spur gears based on genetic algorithm and random forest, Mechanical Systems and

Signal Processing, Volumes 70–71, 2016, Pages 87-103, ISSN 0888 3270, https://doi.org/10.1016/j.ymssp.2015.08.030.

[50] A. Verikas, A. Gelzinis, M. Bacauskiene (2011), Mining data with random forests: A survey and results of new tests, Pattern Recognition, Volume 44, Issue 2, 2011, Pages 330-349, ISSN 0031-3203, https://doi.org/10.1016/j.patcog.2010.08.011.

[51] S. S. Chawathe (2019), Condition Monitoring of Hydraulic Systems by Classifying Sensor Data Streams, 2019 IEEE 9th Annual Computing and Communication Workshop and Conference (CCWC), Las Vegas, NV, USA, 2019, pp. 0898-0904, doi: 10.1109/CCWC.2019.8666564.

[52] Manuel Fernández-Delgado, Eva Cernadas, Senén Barro, Dinani Amorim (2014), Do we Need Hundreds of Classifiers to Solve Real World Classification Problems? JMLR, 15(90):3133−3181, 2014.

[53] Li L, Huang Y, Tao J, Liu C. (2019), Internal leakage identification of hydraulic cylinder based on intrinsic mode functions with random forest. *Proceedings of the Institution of Mechanical Engineers, Part C: Journal of Mechanical Engineering Science*. 2019;233(15):5532-5544. doi:10.1177/0954406219846148

[54] Jatin Prakash (2022) Intelligent methods of supervised and semi supervised learning for health monitoring of hydraulic systems. PhD Dissertation, Indian Institute of Technology Indore.